

This is an Open Access document downloaded from ORCA, Cardiff University's institutional repository: <https://orca.cardiff.ac.uk/id/eprint/102944/>

This is the author's version of a work that was submitted to / accepted for publication.

Citation for final published version:

Mohammed, Aya and Babatunde, A. O. 2017. Modelling heavy metals transformation in vertical flow constructed wetlands. *Ecological Modelling* 354 , pp. 62-71. 10.1016/j.ecolmodel.2017.03.012

Publishers page: <http://dx.doi.org/10.1016/j.ecolmodel.2017.03.012>

Please note:

Changes made as a result of publishing processes such as copy-editing, formatting and page numbers may not be reflected in this version. For the definitive version of this publication, please refer to the published source. You are advised to consult the publisher's version if you wish to cite this paper.

This version is being made available in accordance with publisher policies. See <http://orca.cf.ac.uk/policies.html> for usage policies. Copyright and moral rights for publications made available in ORCA are retained by the copyright holders.



1 **Modelling heavy metals transformation in vertical flow constructed wetlands**

2 **A. Mohammed^{a, b,*} and A. O. Babatunde^{a,c}**

3
4 ^aHydro- environmental Research Centre, Energy and Environment Theme, Cardiff University
5 School of Engineering, Queen's Buildings, The Parade, CF24 3AA, Cardiff, Wales, UK.

6 ^bSouthern Technical University, Basrah Engineering Technical College, Basrah, Iraq.

7 ^cInstitute of Public Health and Environmental Engineering, School of Civil Engineering,
8 University of Leeds, Leeds LS2 9JT, UK.

9 *Corresponding author: e-mail: MOHAMMEDAA2@cardiff.ac.uk

10 Abstract

11 Constructed wetlands are dynamic ecosystems for which we generally have poor predictive
12 capabilities of the succession relationships between the interdependent components and the
13 processes. In this study a dynamic simulation model that can evaluate the transport and fate
14 of heavy metals in vertical flow constructed wetland systems was developed using a dynam-
15 ic software program: Structural Thinking Experiential Learning Laboratory with Animation
16 (STELLA) v9.0.2. The key heavy metals transformation processes considered in the study
17 were adsorption and plant uptake; whilst the forcing functions considered were wastewater
18 volume, temperature, heavy metals concentration, contact time, flow rate and adsorbent
19 media. The model results indicate that up to 89%, 91% and 91% of Pb, Cr and Cd respec-
20 tively, can be removed through adsorption process; whereas uptake by plants was 6%, 5.1%
21 and 5.2% based on mass balance calculations. Sensitivity analysis also showed that the
22 most sensitive areas in the model coincide with the adsorption parameter (the heterogeneity
23 factor (n) and the Freundlich constant (Kf)). The results obtained indicates that the model
24 can be used to simulate outflow heavy metal concentrations, and it can also be used to es-
25 timate the amount of heavy metal removed by individual processes in the system.

26 **Keywords:** Constructed wetland, ferric sludge, heavy metals, STELLA.

27 1. Introduction

28 Constructed wetland systems (CWs) have become a popular technical alternative worldwide
29 for the treatment of various wastewaters. (Kadlec and Wallace, 2008). They are used not
30 only to degrade organic substances and nutrients from wastewaters (Sun and Austin, 2007;
31 Sun et al., 2005), but also to remove metals from several industrial wastewaters (Cheng et
32 al., 2002; Zhao et al., 2009).

33 Unlike organic pollutants, heavy metals (HM) cannot be degraded through biological pro-
34 cesses. Understanding the mechanism of HM removal has expanded concurrently with in-
35 creased adoption and usage of treatment wetlands (Kosolapov et al., 2004). Marchand et al.
36 (2010) indicated that there are four main processes of metals removal in CWs. These in-
37 clude adsorption to fine textured sediments and organic matter; precipitation as insoluble
38 salts (mainly sulphides and oxyhydroxides); absorption and induced changes in biogeo-
39 chemical cycles by plants and bacteria; and deposition of suspended solids due to low flow
40 rates.

41 However, adsorption represents an important mechanism for removal of metals in CWs.
42 Therefore, to ensure efficient HM removal, it is important to use substrates with high HM re-
43 moval capacity and suitable physiochemical properties. A low-cost material that can en-
44 hance HM removal is ferric dewatered sludge (Mohammed et al., 2016). It is available
45 worldwide and is mostly landfilled at huge costs since it is regarded as a waste with little
46 known reuse value. However, the physicochemical properties of ferric dewatered sludge give
47 it a highly reactive surface and a strong affinity for phosphorous and HM (Al-Tahmazi and
48 Babatunde, 2016; Mohammed et al., 2016).

49 Plants also play an important role in CWs for the removal of pollutants. They take up nutri-
50 ents and they are also able to adsorb and accumulate metals (Cheng et al., 2002). Moreo-
51 ver, *Phragmites australis*, known as common reed, is widely used in CWs for treatment of
52 urban and industrial wastewaters containing metals (Bonanno and Lo Giudice, 2010).

53 The efficiency of CWs for wastewater treatment is often evaluated by a comparison between
54 influent and effluent. However, this is a figurative black- box approach since there is no in-
55 formation on the biological and physicochemical processes occurring in the CWs Modelling
56 of HM removal in CWSs is important with regards to understanding the HM behaviour in the
57 integrated treatment processes. Various modelling tools including FITOVERT, CW2D,
58 PHWAT and CWM1 have been used to understand the processes in CWSs (Kumar and
59 Zhao, 2011). However, all these models have been used to simulate the hydraulic properties
60 or degradation of pollutant. In this study the fate of Pb, Cr and Cd in a vertical flow con-
61 structed wetland (VFCW) was investigated through the development of a mathematical
62 model using the Structural Thinking Experiential Learning Laboratory with Animation (STEL-
63 LA) v9.0.2 software. The key objectives were: (1) to develop a dynamic model for simulating
64 adsorption, plant uptake and plant growth from the VFCW which uses ferric dewatered
65 sludge as main substrate; (2) to calibrate the model using the available experimental data;
66 and (3) to apply the model to simulate the fate of HM in the VFCW.

67 2. Materials and methods

68 2.1. Set-up of vertical flow constructed wetland system

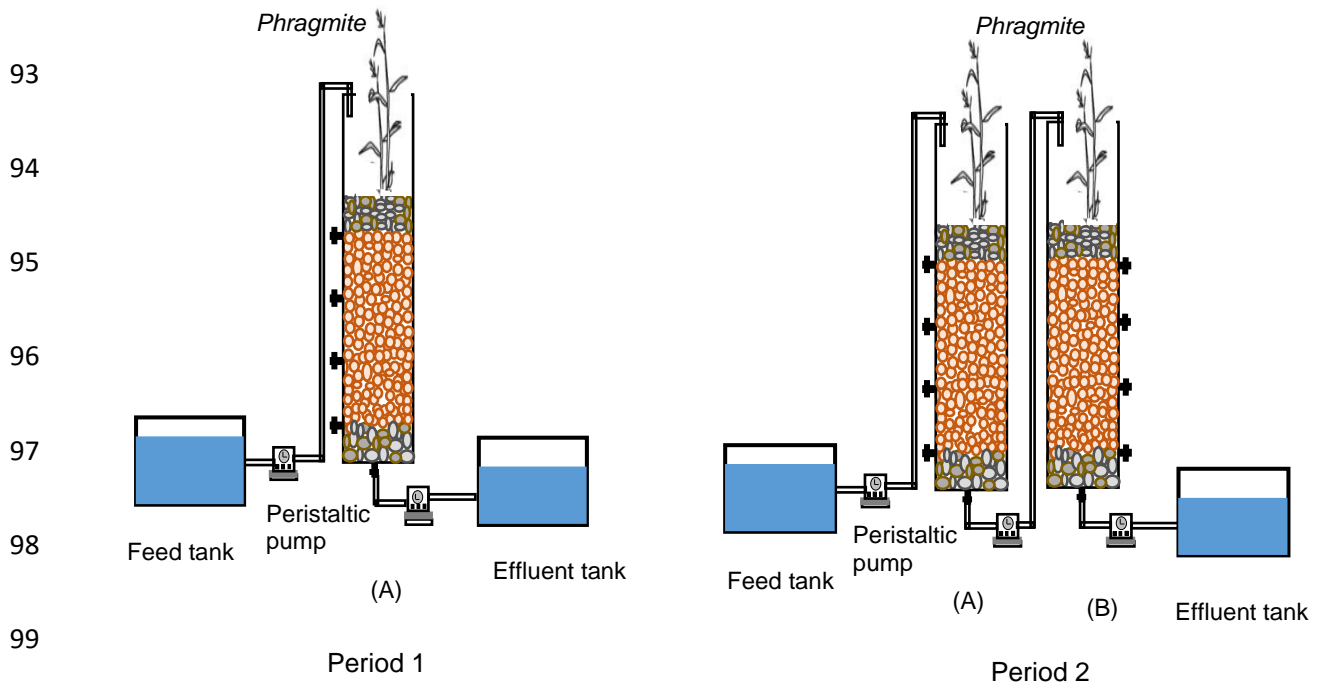
69 A laboratory scale VFCW system was set up outdoor using perspex columns that were 100
70 mm in diameter and 1000 mm in height. Each column was filled with 22 ± 3 mm of round
71 gravel to a depth of 150 mm from the bottom, which served as a drainage layer (see Figure
72 1). Air-dried ferric dewatered sludge with a particle size of 1-3 mm was used as the primary
73 media layer (350 mm), followed by 7 ± 2 mm washed gravel for a depth of 150 mm, giving an
74 average porosity of 0.43. The ferric dewatered sludge consisted of Fe (193.85 mg g^{-1}); its
75 detailed physicochemical properties have been published elsewhere (Mohammed et al.,
76 2016). In brief, the specific surface area was $132 \text{ m}^2 \text{ g}^{-1}$ and the iron oxalate content was
77 162 mg g^{-1} which confirmed the amorphous nature of the ferric dewatered sludge. Each col-
78 umn experienced cyclic wet and dry period with the artificial landfill leachate. These periods
79 were generated by peristaltic pumps. Each wet cycle was completed in three hours and fifty

80 minutes, giving each column 3:50 h of wastewater-media contact per cycle. Common reed,
81 *Phragmites australis*, was planted on the top layer of the stage.

82 Experiments were carried out in two periods, namely Period 1 and 2. The initial purpose of
83 the experiments was to investigate the removal rate of HM from landfill leachate. However,
84 significant removal was not found in the performances of individual CW stages during Period
85 1. Accordingly, alterations to the experiment were made in Period 2. Only one CW stage (re-
86 ferred to as 'A' in Figure 1) was used in Period 1, whereas in Period 2 two CW stages (A +
87 B), which were arranged in parallel, were used.

88 To simulate young landfill leachate, $\text{CdSO}_4 \cdot \text{H}_2\text{O}$ salt, $\text{Cr}(\text{SO}_4)_2 \cdot 12\text{H}_2\text{O}$ salt and PbCl_2 salt,
89 respectively for cadmium (Cd), chromium (Cr) and lead (Pb) were used to synthesise arti-
90 ficial landfill leachate in the laboratory. The initial concentrations of HM were ($230 \mu\text{g L}^{-1}$ - 630
91 $\mu\text{g L}^{-1}$), ($240 \mu\text{g L}^{-1}$ - $650 \mu\text{g L}^{-1}$) and ($240 \mu\text{g L}^{-1}$ - $810 \mu\text{g L}^{-1}$) for Pb, Cr and Cd, respectively.

92



101 Figure 1. Schematic description of the constructed wetland system in Period 1 (left) and Period 2
102 (right).

103

104 2.2. Batch analysis

105 Batch experiments were used to investigate the kinetic of the adsorption process and
106 examine the kinetics of heavy metal adsorption by the ferric dewatered sludge. To
107 investigate the effects of sludge dosage and equilibration time, different masses of the
108 sludge sample (0.1, 0.5 and 1.0 g) were equilibrated with 100 ml each of heavy metal
109 solutions (0.5 mg L⁻¹ for Pb, 1 mg L⁻¹ for Cr and 5 mg L⁻¹ for Cd), which were contained in
110 250 ml polyethylene bottles for 1–96 h using a rotary shaker. At specified time points, the
111 mixture was withdrawn, filtered and analysed for each heavy metal using an Optima 210 DV
112 ICP OES, and the uptake of those metals was determined using Eq. (1).

113

114
$$q_e = \frac{(c_o - c_e)}{m} v \dots\dots\dots(1)$$

115

116 Here, C_o and C_e (both in mg L⁻¹) are the initial (t=0) and final heavy metals concentrations at
117 equilibrium (q_e), respectively; q_e is the mass of heavy metal adsorbed on the adsorbent
118 (sludge) at equilibrium (mg g⁻¹); v is the volume of the solution (L); and m is the mass of
119 ferric dewatered sludge used (g).

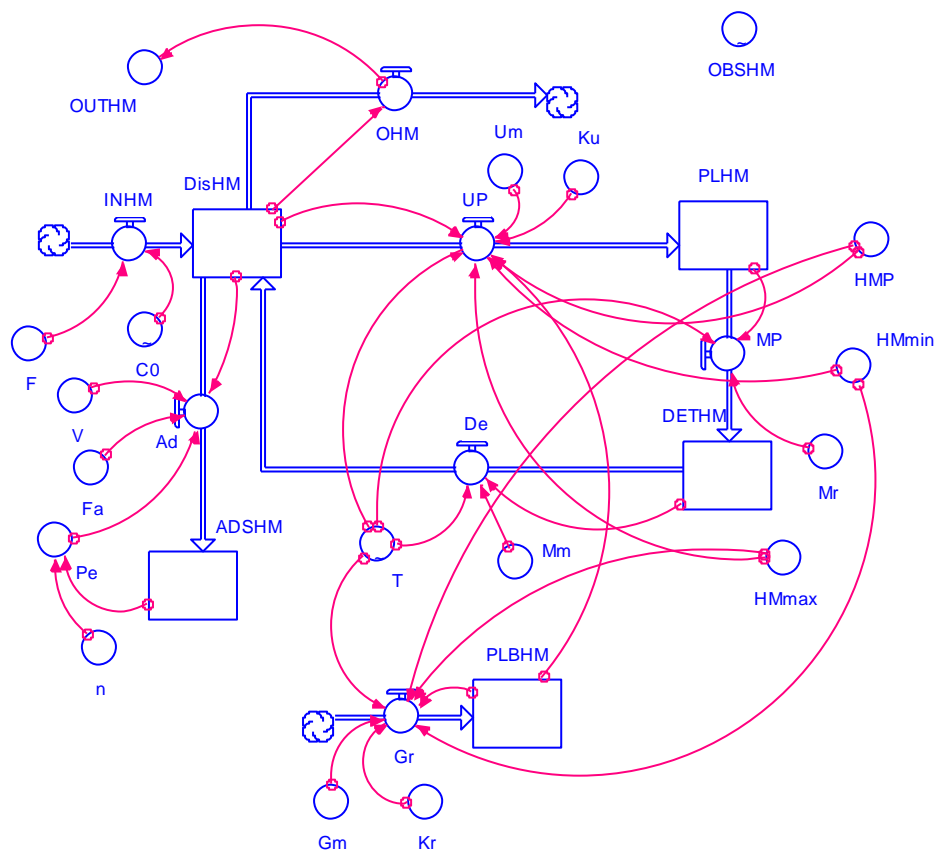
120 2.3. Description of the STELLA model

121 According to Jay Forrester's systems dynamics language, STELLA is a software for graphic
122 and dynamic simulation. The use of iconographic modelling techniques makes the model a
123 flexible simulation tool with an easy user interface for making change and calibrate. The user
124 can immediately view the effects of the changes, which reduces the time required to develop
125 the model (Jørgensen and Fath, 2011).

126 Conceptual diagrams of the adsorption processes, plant uptake and plant growth for Pb, Cr
127 and Cd are shown in the STELLA diagrams below (Figures 2-4). The major mechanisms for
128 HM dynamics in CWS considered in this study were adsorption and plant uptake. The
129 removal of heavy metals in CWs is widely attributed to adsorption and plant uptake
130 (Kosolapov et al., 2004; Marchand et al., 2010). The developed models have five state

131 variables including dissolved HM (DISHM), plant HM (PLHM), which means the heavy
 132 metals that are available for plant uptake are those that are present as soluble components
 133 in the soil solution or those that are easily solubilized by root exudates, Although plants
 134 require certain heavy metals for their growth and upkeep so that the third state is plant
 135 biomass (PLBHM), detritus HM (DETHM) and adsorption (ADSHM), all expressed in mg of
 136 HM per day. Adsorbent HM concentration and contact time are considered to be major
 137 forcing functions in the model, since the adsorption process is highly related to the retention
 138 capacity of substrates over time (Marchand et al., 2010). The state variables, processes,
 139 parameters and auxiliary variables used in the model are shown in Table 1. Detailed
 140 descriptions of each mechanism responsible for removal and HM dynamics are presented
 141 below.

142



143

144

Figure 2. A STELLA diagram of the HM model.

145

146 2.3.1. Process equations

147 The adsorption process was described by the equilibrium between HM in water and HM in
 148 the adsorbent. Unlike other processes, this process is fast and reaches equilibrium in hours,
 149 based on the batch results (Figure 9). Therefore, 0.02 delta time (DT) was selected as the
 150 time step. DT refers to the time interval between calculations in STELLA software. In addi-
 151 tion, the adsorption process was multiplied by a factor (Fa) of 2.5, 5 and 3, respectively for
 152 Pb, Cr and Cd for column A, and 3.5, 14 and 5, respectively for Pb, Cr and Cd for column B.
 153 These factors were based on experimental results, and it is expected that they will vary ac-
 154 cording to the type of media, HM concentrations, type of pollutant, type of CWs, etc.
 155 Adsorption process can be describe using equation 2, where, Fa is a factor, $DISHM$ is
 156 dissolve HM (either Pb, Cr or Cd) (mg day^{-1}), P_e is the equilibrium concentration ($\text{mg L}^{-1} \text{ day}^{-1}$)
 157 and V is the volume of wastewater (L).

158

159 $Ad = Fa(DISHM - P_e \times V)$(2)
 160

161 P_e can be calculated by using equation 3, where $ADSHM$ is adsorption of HM (either Pb, Cr
 162 or Cd) (mg day^{-1}), T_A is the total amount of adsorbent (g), K_F is the Freundlich constant (L g^{-1})
 163 and n is the heterogeneity factor.

164 $P_e = \left(\frac{ADSHM}{T_A \times K_F} \right)^n$(3)
 165

166 Mohammed et al. (2016) found that the Freundlich adsorption model was well fit to describe
 167 the adsorption behaviour of Pb, Cr and Cd, with correlation coefficients of 0.97, 0.98 and
 168 0.98 for Pb, Cr and Cd, respectively.

169 The growth of the plant, *phragmites australis* depends on the amount of HM in the plant and
 170 can be described as a function of maximum growth rate at the optimum temperature.

171 Furthermore, the plant's growth can be expressed by Michaelis-Menton equation of
 172 dissolved HM. The following equation was used to describe plant growth:

173

$$174 \quad Gr = \frac{G_m \times PLB \times (HM_p - HM_{min}) \times 1.05^{(T-20)}}{K_r \times (HM_{max} - HM_{min})} \dots\dots\dots(4)$$

175

176 Here, G_m and K_r are maximum HM growth rate of the plant and the plant's growth rate
 177 (Michaelis-Menton half saturated constant for growth); PLB is plant biomass; HM_p , HM_{min}
 178 and HM_{max} are heavy metal in the plant, minimum heavy metal in the plant and maximum
 179 heavy metal in the plant, respectively; and T is temperature. Plant uptake (*phragmites*
 180 *australis*) is defined as a function of maximum uptake rate at the optimum temperature as
 181 explained in equation 5, where U_m and K_u are the maximum uptake rates of plants and the
 182 uptake rate of HM (Michaelis-Menton half saturated constant for uptake), respectively.

183

$$184 \quad Up = \frac{U_{max} \times PLB \times (HM_{max} - HM_p) \times DISHM \times 1.05^{(T-20)}}{(DISHM - K_u) \times (HM_{max} - HM_{min})} \dots\dots\dots(5)$$

185

186 The first order reaction with Arrhenius function of temperature was used to express the plant
 187 mortality and the detritus and as shown below.

188

$$189 \quad MHM = PLHM \times M_r \times 1.07^{(T-20)} \dots\dots\dots(6)$$

190

$$191 \quad De = DETHM \times M_m \times 1.07^{(T-20)} \dots\dots\dots(7)$$

192

$$193 \quad KT = K_{20} \theta^{(T-20)} \dots\dots\dots(8)$$

194

195 Here, M_r and M_m are the mortality rate and maximum HM mineralization, respectively; KT is
 196 the removal rate constant at $T^\circ\text{C}$; K_{20} is the removal rate constant at 20°C ; θ is

197 dimensionless; and T is the water temperature ($^{\circ}\text{C}$). The value of θ is 1.05 for plant growth
198 and plant uptake, whereas the plant's mortality decomposition is more sensitive to
199 temperature changes. Therefore, the θ value ranges from 1.07 to 1.08 (Kumar et al., 2011).

200 2.4. Calibration and sensitivity analysis

201 Before applying the resulting STELLA model to estimate the removal of heavy metals, the
202 model was calibrated and validated using a standard trial and error procedure. In general,
203 model calibration is a process adjusting the selected parameter values to obtain the best fit
204 between the observed data and simulated results. In practical modelling, sensitivity analysis
205 is carried out to aid in model calibration. This is done by changing the parameters and
206 observing the corresponding response on the selected parameter. Thus, the sensitivity (S) of
207 a parameter (P) is defined as follows:

$$208 \quad S = \frac{\delta X / X}{\delta P / P} \dots\dots\dots(9)$$

209
210 Here, X is the model output. The higher the value of S , the more important the parameter
211 (Jørgensen and Fath, 2011). The relative change in the parameter is chosen based on
212 experimental knowledge as to the certainty of the parameters.

213 Table 1. Summary of the state variables, processes, parameters and their associated units in the model development for Pb, Cr and Cd.

Symbol	Description	Value	Unit	Source		
State variables						
ADSHM	Amount of HM adsorbed in ferric dewatered sludge	-	mg HM day ⁻¹	Calculated		
DISHM	Dissolved amount of HM in ferric dewatered sludge	-	mg HM day ⁻¹	Observed data		
PLHM	Amount of HM found in plants	-	mg HM day ⁻¹	Estimated		
PLBHM	Amount of HM found in plants biomass	-	mg HM day ⁻¹	Estimated		
DETHM	Amount of HM found in detritus and used by bacteria	-	mg HM day ⁻¹	Estimated		
Processes						
Gr	HM requirement for growth	Eq.(4)	mg HM day ⁻¹	-		
Up	HM through plants	Eq.(5)	mg HM day ⁻¹	-		
Mp	Mortality of plant	Eq.(6)	mg HM day ⁻¹	-		
De	Decomposition of detritus	Eq.(7)	mg HM day ⁻¹	-		
Ad	HM adsorption	Eq.(2)	mg HM day ⁻¹	-		
Parameters		Pb	Cr	Cd		
HMmax	Maximum HM in plants	0.11	1	1.5	g (100g) ⁻¹	Estimated
HMmin	Minimum HM in plants	0.001	0.195	0.016	g (100g) ⁻¹	Estimated
Um	Maximum uptake of HM from plants	0.26	0.114	0.09	mg HM (L day) ⁻¹	Calculated
Ku	Michaelis Menton for uptake	5.24	2.18	2	day ⁻¹	Calculated
Mm	Maximum mineralization	0.2	0.2	0.2	day ⁻¹	(Kumar et al., 2011)
Pe	HM equilibrium concentration				mgHM (L day) ⁻¹	Calculated

HMp	HM in plant	-	-	-	mg mg ⁻¹	Calculated
		0.000024	0.00052	0.00002		Kumar et al., 2011)
Mr	Mortality rate				mg HM (L day) ⁻¹	Calculated
		0.001	0.001	0.001		Calculated
Gm	Maximum growth of plant				mg day ⁻¹	Calculated
Kr	Michaelis Menton plant growth rate	5.8	4.3	2	mg HM (L day) ⁻¹	
		3.8	2.6	0.45		
Others						
INHM	Inflow of HM	TF			mgHM day ⁻¹	Observed data
C ₀	HM concentration of inflow	TF			mgHM L ⁻¹	Observed data
T	Temperature requirement of plant growth	TF			°C	Observed data
V	Volume of wastewater	12			L	Experiment
F	Flow rate of wastewater into the CW	12			L day ⁻¹	Experiment
TA	Amount of adsorbent	2500			g	Calculated

214 TF is a Table function which is incorporated into the model.

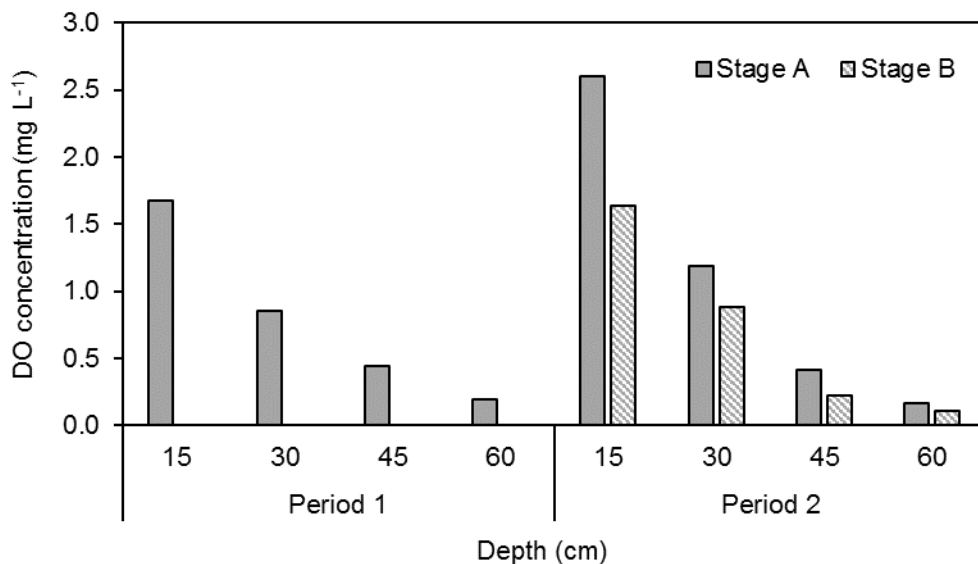
215 3. Result and discussion

216 3.1. Simulation of heavy metals using STELLA software

217 Experiments were carried out for two periods using column A (215 days) for Period 1 and
218 columns A and B (185 days) for Period 2. A comparison of the measured and modelled data
219 was undertaken using Period 1 for calibration and Period 2 for validation. During the
220 calibration, the input parameters were obtained from experimental measurements,
221 theoretical calculations or existing literature (Table 1). The model was calibrated by trial and
222 error adjustment of the key parameters (within a reasonable range) until predictions under
223 similar conditions had good agreement with the observed data. The measured HM
224 concentrations ranged from 54 $\mu\text{g L}^{-1}$ - 264 $\mu\text{g L}^{-1}$, 21 $\mu\text{g L}^{-1}$ - 190 $\mu\text{g L}^{-1}$ and 87 $\mu\text{g L}^{-1}$ - 342 $\mu\text{g L}^{-1}$,
225 L^{-1} , respectively, for Pb, Cr and Cd. Whereas the simulation ranged from 92 $\mu\text{g L}^{-1}$ - 255 $\mu\text{g L}^{-1}$,
226 1 , 38 $\mu\text{g L}^{-1}$ - 262 $\mu\text{g L}^{-1}$ and 80 $\mu\text{g L}^{-1}$ -324 $\mu\text{g L}^{-1}$, respectively, for Pb, Cr and Cd during the
227 calibration period. The maximum value of the measured effluent concentration (OBS) for all
228 of the HM was very close to the value simulated by the STELLA model. However, the
229 predicted data were slightly higher than the measured data for all of the HM, with the
230 exception of a few data points. In addition, the model did not simulate very low values for all
231 of the HM. Figure 4 shows the entire trend of model calibration and validation for column A.
232 The mean percent error ($\text{MPE} = (\text{OBS} - \text{OUT})/\text{OBS} \times 100$) equals 38%, 33% and 30%,
233 respectively, for Pb, Cr and Cd during the calibration period, and 15%, 20% and 10%,
234 respectively, for Pb, Cr and Cd during the validation period. It is worth noting that the
235 validated data for the HM was quite close to the observed data, despite the fact that the
236 simulation data was higher than the observation data for the period of 320- 400 days (during
237 validation between 105 and 185 days in period 2) in the case of Cr. This slight fluctuation in
238 the model simulation and the experimental data could be due to experimental error or
239 accumulation of biomass within the CWs (growth of microorganism). This could also be
240 attributed to the fact that the plants were not harvested during the experimental period. The
241 uptake of HM by plant is a step function during the growing season and zero after harvest

242 until the next growing season start (Jørgensen and Fath, 2011). However, the contribution of
 243 plant harvesting is a small percent to the total HM removal in CWs, so that it is ignore in this
 244 study (Cheng et al., 2002; Kosolapov et al., 2004; Marchand et al., 2010).

245 . Another possible reason may be that apart from the adsorption process, the HM in CW can
 246 be removed by other processes, such as precipitation, oxidation, ion exchange and redux
 247 reaction (Galletti et al., 2010). However, the system was operated to be fully saturated for
 248 3:50 hours and unsaturated for 10 minute and due to a limitation of DO diffusion within HH
 249 sludge (Wang et al., 2008), there is aerobic and anaerobic condition along the height of the
 250 column as shown in figure (3). Therefore, the co-precipitation of HM with Fe oxide is very
 251 dependent on DO variations so that the binding of metals with Fe oxide cannot be a long-
 252 term removal mechanism, and then metals may be released back to the system. Moreover,
 253 Fe oxide high affinity to metals that have similar size of Fe such as Cd, however the co-
 254 precipitate is limited when there is sufficient amount of SO_4 which reducing the potential of
 255 metal removal (Marchand et al., 2010). In addition, under anaerobic condition and because
 256 of there is no sufficient carbon source required by sulphate- reducing bacteria to sulphides,
 257 precipitation metals as metal sulphide cannot occur (Stefanakis et al., 2014).



258

259 Figure 3 Vertical initial DO distribution at different depth (from top layer to bottom) in four
 260 stages of constructed wetland system.

261

262 A comparison of the observed and predicted Pb, Cr and Cd concentration values in the
263 effluent during the model calibration process obtained using linear regression is shown in
264 Figure 5. The R^2 values for Pb, Cr and Cd outlet concentration values were 0.75, 0.69 and
265 0.62, respectively. The R^2 values for comparisons of the observed and predicted Pb, Cr and
266 Cd outlet concentration values during the model validation process (Figure 6) were 0.78,
267 0.65 and 0.74, respectively for Pb, Cr and Cd concentration. These values represent good
268 correlations between the model predictions and the experimental measurements.

269 Based on these results, the mathematical model developed in this study could be used to
270 describe the HM removal process in the VFCW using ferric dewatered sludge as the primary
271 media. The model was run using STELLA software for a period of 185 days for column B.
272 Since the results of the validation data in column A displayed a good match between simu-
273 lated and experimental data, the calibration for column B was performed with the column A
274 data. The experimental effluent HM concentrations ranged from 25 $\mu\text{g L}^{-1}$ to 76 $\mu\text{g L}^{-1}$, 8 μg
275 L^{-1} to 22 $\mu\text{g L}^{-1}$ and 24 $\mu\text{g L}^{-1}$ to 76 $\mu\text{g L}^{-1}$, respectively for Pb, Cr and Cd. On the other hand,
276 the simulation data for Pb, Cr and Cd ranged, respectively, from 23 $\mu\text{g L}^{-1}$ to 63 $\mu\text{g L}^{-1}$, 11 μg
277 L^{-1} to 24 $\mu\text{g L}^{-1}$ and 27 $\mu\text{g L}^{-1}$ to 68 $\mu\text{g L}^{-1}$, as shown in Figure 7. This figure shows that the
278 mean concentration values of HM for the measured and simulated values were very close
279 and, therefore, the overall simulation is acceptable for column B. The MPEs for this column
280 were 17% for Pb, 17% for Cr and 17% for Cd. A comparison between the observed and
281 predicted Pb, Cr and Cd concentrations in effluent during the model validation process for
282 column B showed good correlations between the model predictions and the experimental
283 measurements, with R^2 being 0.82, 0.71 and 0.76, respectively, for the Pb, Cr and Cd outlet
284 concentrations (Figure 8).

285

286

287

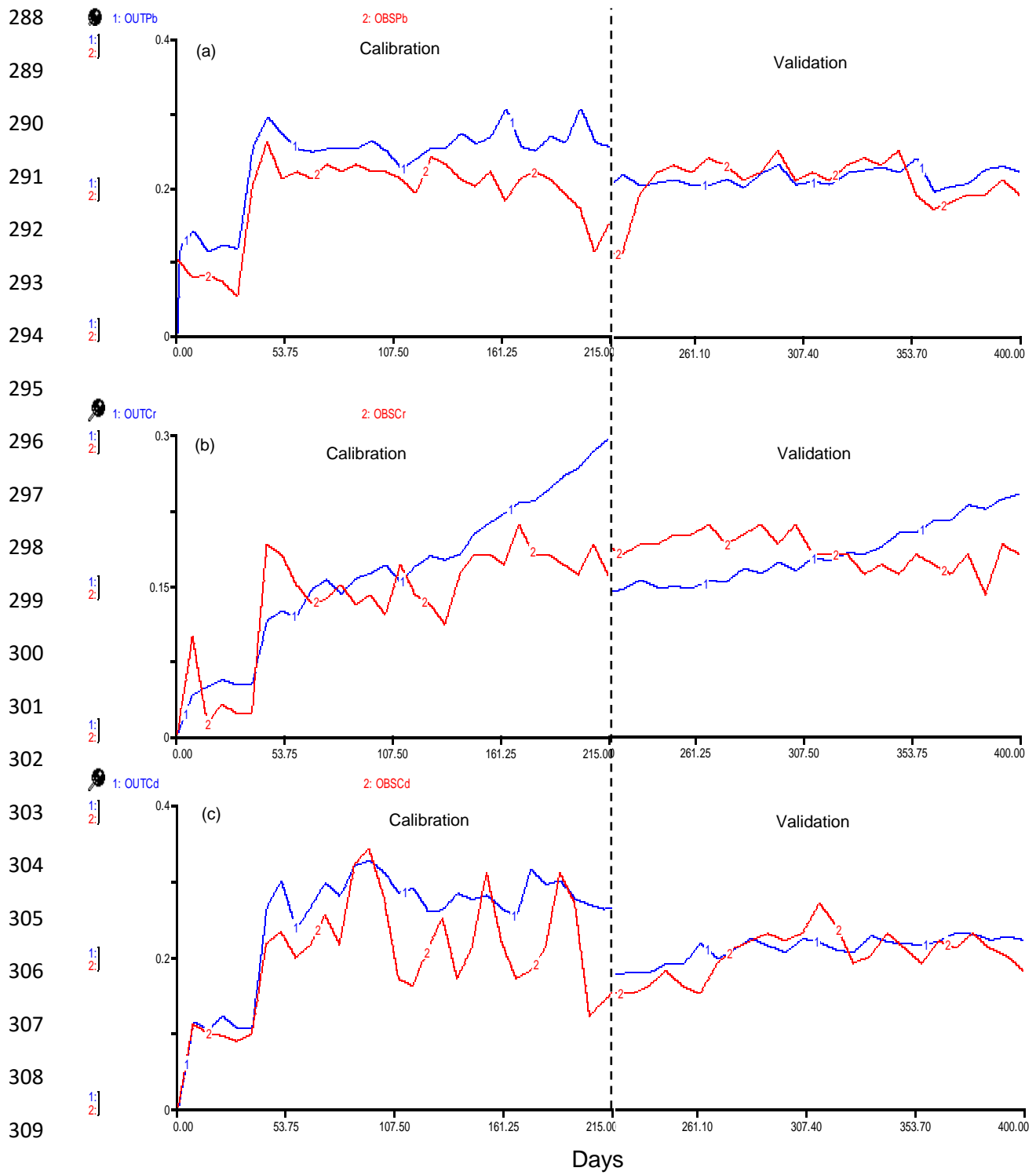


Figure 4. Model calibration and validation for (a) Pb, (b) Cr and (c) Cd removal in mg L^{-1} in VFCW for column A.

316
317
318
319
320
321
322
323
324
325
326
327
328
329
330
331
332
333
334
335
336
337
338
339
340

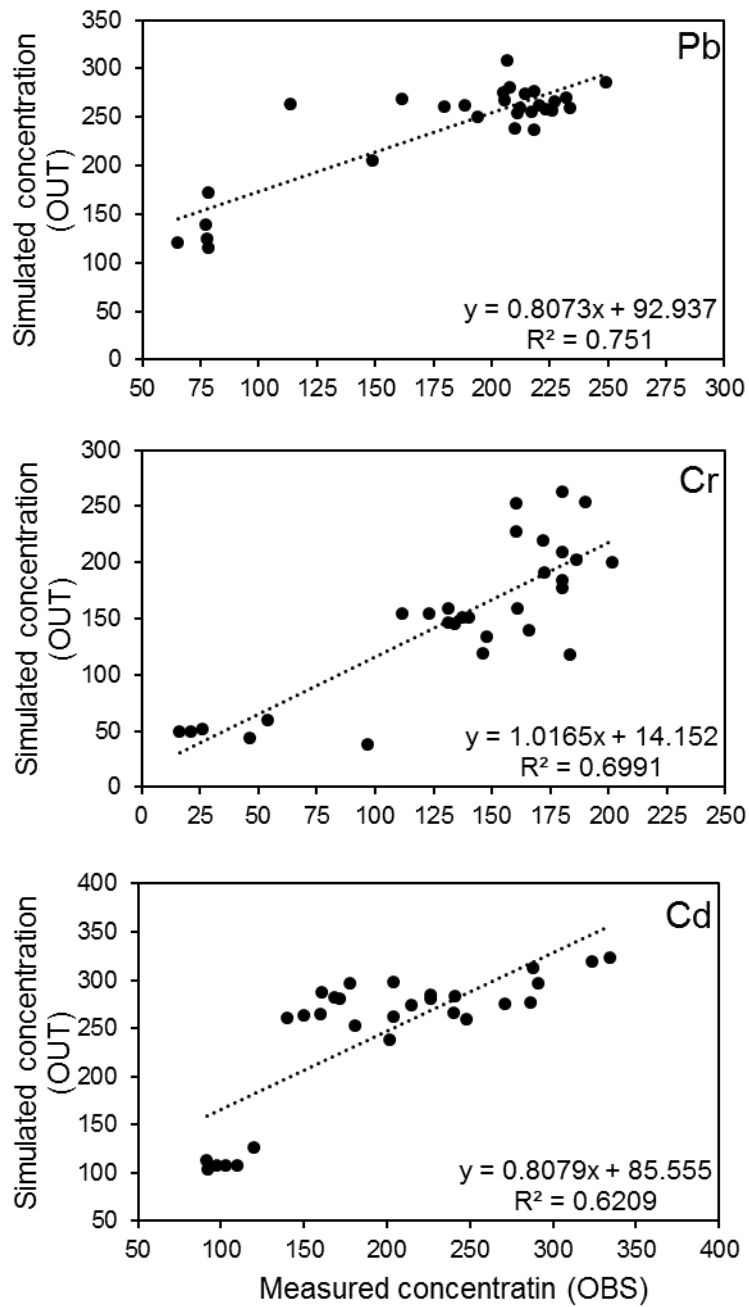


Figure 5. Comparison of model predicted and field measured of Pb, Cr and Cd removal in $\mu\text{g L}^{-1}$ in VFCW for column A during model calibration.

341
342
343
344
345
346
347
348
349
350
351
352
353
354
355
356
357
358
359
360
361
362
363
364

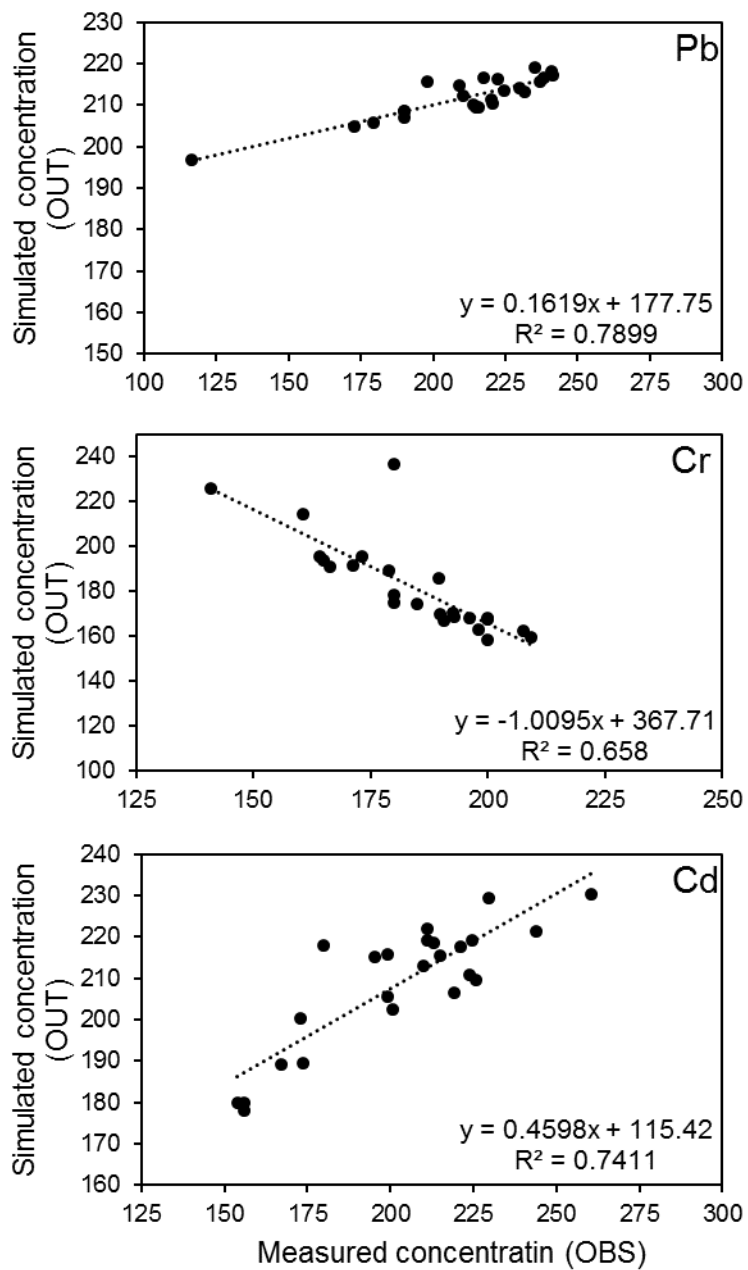
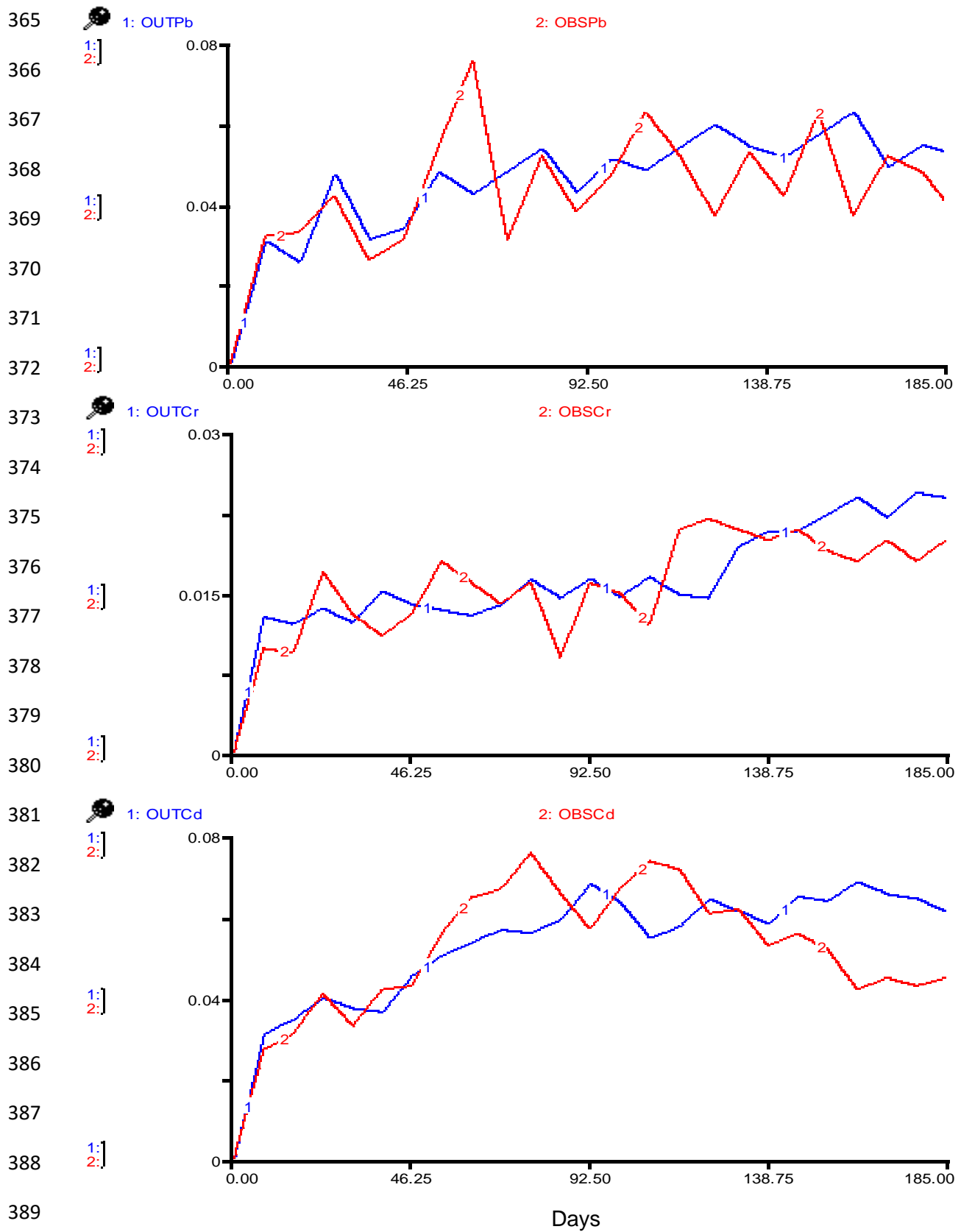


Figure 6. Comparison of model predicted and field measured of Pb, Cr and Cd removal in $\mu\text{g L}^{-1}$ in VFCW for column A during model validation.



390 Figure 7. Model validation for (a) Pb, (b) Cr and (c) Cd removal in mg L^{-1} in VFCW for column B.

392
393
394
395
396
397
398
399
400
401
402
403
404
405
406
407
408
409
410
411
412
413
414

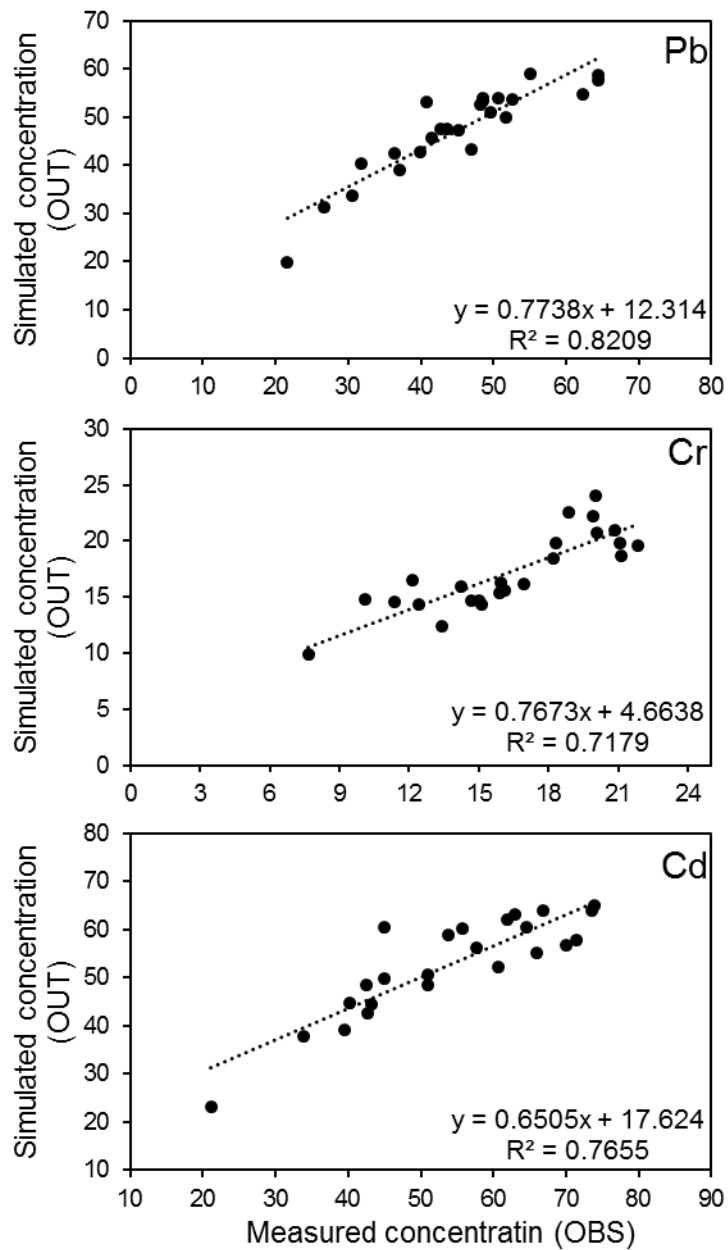


Figure 8. Comparison of model predicted and field measured of Pb, Cr and Cd removal in μgL^{-1} in VFCW for column B during model validation.

415 3.2. Sensitivity analysis

416 A sensitivity analysis provides a good overview of the most sensitive components in the
417 model. This type of analysis attempts to provide a measure of the sensitivity of the parame-
418 ters by forcing functions, initial values of the state variables of the sub models, to the state
419 variables of greatest interest in the model (Jørgensen and Fath, 2011). The sensitivity of the
420 model was tested using the 10 parameters which were most likely to be important: G_m , K_r ,
421 U_m , K_u , M_m , M_r , HM_{max} , HM_{min} , n and K_f (Table 2). This was done by examining the rela-
422 tive change in the model output and dividing it by the relative change in the value of the test-
423 ed parameter. The magnitude of the changes in the parameter values may be proportional to
424 the value of the parameter; this also depended on the possible range of the parameter. Most
425 changes were made between -50% and +50% (van der Peiji and Verhoeven, 1999). In this
426 study, changes were made at $\pm 40\%$. Table 2 shows that the increase and decrease of n
427 caused a significant change in the corresponding state variable of the model. Similarly, the
428 change in K_f also caused changes in the model output and the corresponding state varia-
429 bles. This is primarily because the adsorption process supposes that the main process for
430 the removal of HM by ferric dewatered sludge in the CWs. The rigid structure and fixed set of
431 parameters do not accurately reflect the changes in the output of VFCW.

432 Table 2. Sensitivity analysis for the selected parameters included in the model.

Change of	Parameter value			S (+40%)			S (-40%)		
	Pb	Cr	Cd	Pb	Cr	Cd	Pb	Cr	Cd
Gm	2.08	3	0.82	1.08×10^{-8} - 1.33×10^{-7}	2.18×10^{-8} - 1.43×10^{-7}	1.64×10^{-7} - 3.22×10^{-7}	2.10×10^{-8} - 1.32×10^{-7}	2.18×10^{-7} - 6.23×10^{-7}	7.08×10^{-8} - 2.47×10^{-7}
Kr	2.8	3	1.26	1.43×10^{-8} - 2.1×10^{-8}	1.98×10^{-7} - 2.13×10^{-6}	1.08×10^{-8} - 2.33×10^{-8}	1.08×10^{-8} - 1.33×10^{-7}	1.11×10^{-7} - 5.01×10^{-6}	2.08×10^{-7} - 4.91×10^{-7}
Um	0.26	0.114	0.09	1.48×10^{-5} - 3.69×10^{-5}	0.41×10^{-5} - 0.55×10^{-3}	6.63×10^{-6} - 2.02×10^{-5}	1.56×10^{-5} - 3.92×10^{-5}	0.41×10^{-3} - 0.55×10^{-3}	6.63×10^{-6} - 2.02×10^{-5}
Ku	5.24	2.18	2	3.91×10^{-6} - 2.38×10^{-5}	0.19×10^{-3} - 0.33×10^{-3}	2.14×10^{-6} - 1.00×10^{-5}	1.41×10^{-5} - 4.72×10^{-5}	0.31×10^{-3} - 0.63×10^{-3}	2.71×10^{-6} - 1.47×10^{-5}
HMmax	0.11	1	1.5	2.01×10^{-5} - 8.75×10^{-5}	6.67×10^{-5} - 8.93×10^{-5}	5.08×10^{-8} - 1.55×10^{-7}	1.45×10^{-5} - 6.33×10^{-5}	0.19×10^{-3} - 0.26×10^{-3}	1.19×10^{-7} - 3.65×10^{-7}
HMmin	0.001	0.195	0.016	2.32×10^{-5} - 0.11×10^{-3}	0.11×10^{-3} - 0.15×10^{-3}	7.17×10^{-8} - 2.18×10^{-7}	8.83×10^{-9} - 3.51×10^{-7}	0.15×10^{-5} - 0.12×10^{-3}	7.12×10^{-8} - 2.16×10^{-7}
Mr	0.001	0.001	0.001	2.48×10^{-6} - 8.48×10^{-6}	7.73×10^{-5} - 0.18×10^{-3}	1.32×10^{-6} - 5.97×10^{-6}	2.67×10^{-6} - 8.61×10^{-6}	8.03×10^{-5} - 0.18×10^{-3}	1.41×10^{-6} - 6.09×10^{-6}
Mm	0.2	0.2	0.2	1.16×10^{-5} - 9.86×10^{-5}	1.82×10^{-6} - 4.72×10^{-5}	5.84×10^{-8} - 8.68×10^{-6}	1.09×10^{-7} - 1.16×10^{-5}	5.05×10^{-6} - 0.10×10^{-3}	1.41×10^{-6} - 6.09×10^{-6}
n	0.53	1.52	0.5	0.60×10^{-1} - 2.00×10^{-1}	2.72×10^{-3} - 3.36×10^{-1}	1.32×10^{-1} - 3.20×10^{-1}	3.10×10^{-1} - 6.41×10^{-1}	4.70×10^{-3} - 5.91×10^{-1}	2.03×10^{-1} - 6.70×10^{-1}
Kf	43	1.7	0.43	0.12×10^{-1} - 0.54×10^{-1}	1.4×10^{-3} - 4.44×10^{-1}	0.3×10^{-1} - 1.43×10^{-1}	0.23×10^{-1} - 1.03×10^{-1}	7.50×10^{-3} - 22.70×10^{-1}	5.00×10^{-1} - 2.60×10^{-1}

433

434 3.3. Fate of heavy metals in VFCW

435 To assess the performance of the VFCW for the removal of HM from landfill leachate, a sim-
436 ulation scenario investigated the HM dynamics for the anoxic condition using ferric de-
437 watered sludge as the primary media in the VFCW. The input data of the HMs were inserted
438 into the STELLA software during model calibration and integrated by using the second order
439 Runge-Kutta method with a time step of 0.02 day. Once the model finished its run (i.e., at the
440 end of 215 days), the amount of HM that accumulates into the state variables, and the pro-
441 cesses of the model show how much HM is removed by the individual pathways. Therefore,
442 it is possible to calculate the efficiency of the individual processes, such as Ad (Eq. 2), Up
443 (Eq. 5) and Mp (Eq. 6) and De (Eq. 7). A mass balance for all state variables, as simulated
444 by the model, revealed that approximately 89%, 91% and 91% for Ad; 6%, 5.1% and 5.2%
445 for Up; and 1%, 1.15% and 1% for Mp and De for respectively Pb, Cr and Cd. The results
446 from the mass balance show that the major HM transformation routes in this study were ad-
447 sorption, with a small amount of uptake by the plant. The effect of various parameters on
448 adsorption was studied via batch experiments (Mohammed et al., 2016). The adsorption
449 results of Pb, Cr and Cd ions by ferric dewatered sludge showed a slightly better fit with the
450 Freundlich compared to Langmuir. The Langmuir isotherms data found that ferric dewatered
451 sludge had $40 \mu\text{g g}^{-1}$, $130 \mu\text{g g}^{-1}$ and $30 \mu\text{g g}^{-1}$ adsorption capacity for Pb, Cr and Cd, re-
452 spectively. On the other hand, the Freundlich isotherm results showed that a precipitation
453 reaction may occur for Pb and Cd removal where n values > 1 (Mohammed et al., 2016).
454 Lead and cadmium could precipitate to form insoluble compounds with sulphide in anaerobic
455 zones of CWs (Kadlec and Wallace, 2008). Figure 9 indicates, as per the laboratory batch
456 experiment, a sharp rise in the Pb and Cr removal within the first hour, indicating the instant
457 at which the removal of these HM takes place. This can be adduced to the excess of binding
458 sites on highly accessible surfaces, like particles and macropores. Over time, the curve
459 starts to plateau because the rate of removal is much slower. This is due to the accumulation

460 of metal ions on the binding sites until it reaches equilibrium; and thereafter, sorption would
461 be via intraparticle diffusion in meso- and micropores and/or sorption by the organic matter
462 (Zhou and Haynes, 2011).

463 The adsorption process in STELLA was described in such a way to calculate the P_e concen-
464 tration using the Freundlich isotherm. From the model simulation, approximately 526 μg , 518
465 μg and 640 μg of Pb, Cr and Cd, respectively, adsorbed during the calibration stage of the
466 model run and the corresponding inflow of these heavy metals amounts were 591 μg , 570
467 μg and 712 μg for Pb, Cr and Cd, respectively. The high amount of HM adsorbed by the me-
468 dia was a result of using ferric dewatered sludge as the main substance and an anoxic con-
469 dition to elongate the contact time between the media and HM. The overall simulation of Ad
470 is reasonably good in the STELLA model, especially for the adsorption process.

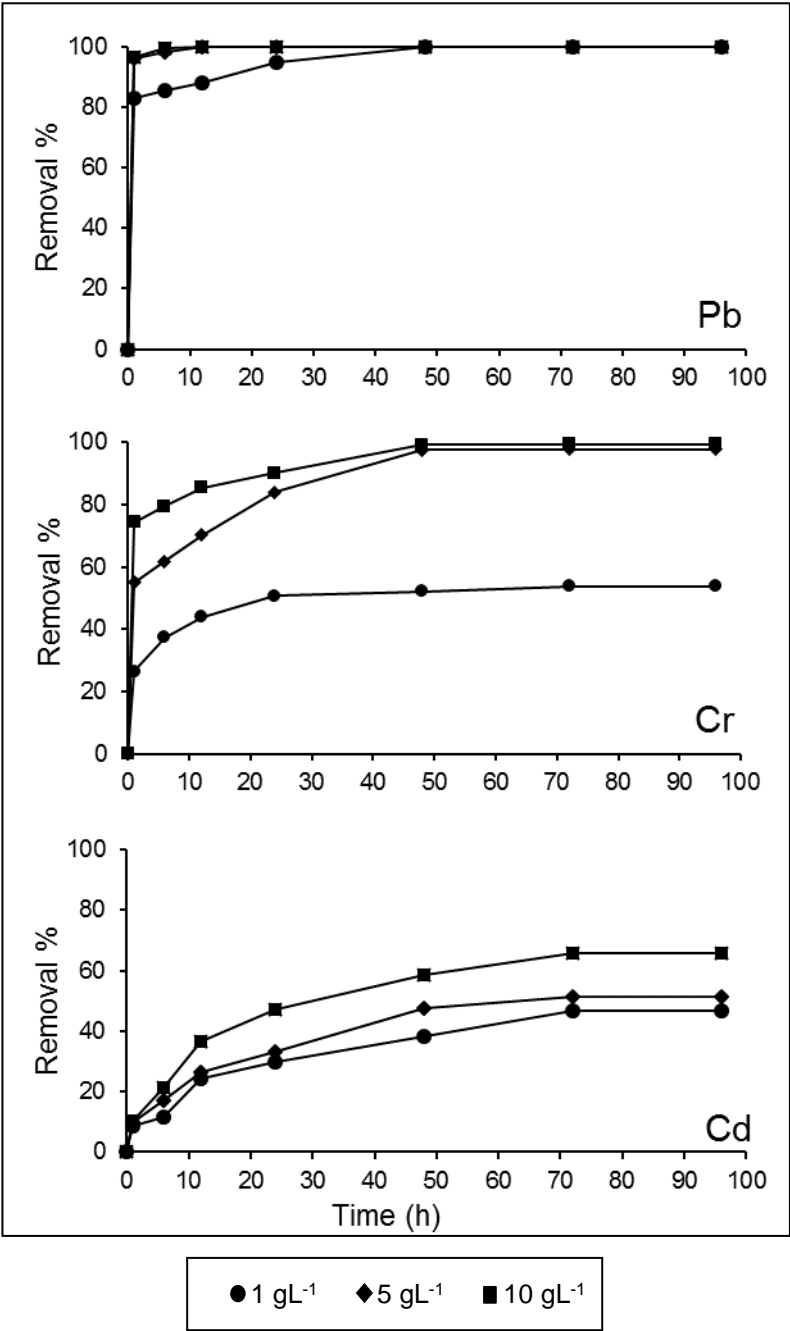
471 Unfortunately, no data from the use of ferric dewatered sludge as a substrate in CWs for HM
472 removal were found in the literature. Therefore, there is no comparison data. However, sev-
473 eral authors used the STELLA program to describe the adsorption process in CWSs and
474 used different kinds of substrate and pollutants. Pimpan and Jindal (2009) show that the
475 maximum cadmium removal simulated by the STELLA software occurred through the accu-
476 mulation in the soil with mass fraction values of 33.6–76.6% at different hydraulic retention
477 times. Kumar et al. (2011) revealed that 72% of phosphorus removed through the adsorption
478 process simulated by the STELLA software using alum sludge and vertical flow constructed
479 wetland. Accordingly, adsorption seems to be the main process to remove Cd and phospho-
480 rous in CWS.

481 The uptake of HM by plants in this study was low. This primarily because the CWs plants
482 can be contribute to HM removal through substrate stabilization, rhizosphere oxidation, the
483 supply of organic matter for microorganism and the transportation of water to wetland soil,
484 rather than through the direct uptake of metals (Kosolapov et al., 2004).

485

486

487
488
489
490
491
492
493
494
495
496
497
498
499
500
501
502



503
504

505 Figure 9. Removal efficiency of heavy metals by ferric dewatered sludge at different sludge dosage
506 and contact time.

507 4. Conclusion

508 In this study, a dynamic model for HM transformation in a vertical flow constructed wetland
509 and using ferric dewatered sludge as main substance was developed using STELLA. The
510 mechanisms used in this modelling process included adsorption, uptake by the plant and

511 plant growth. The most significant pathway of heavy HM retention was adsorption. In terms
512 of the model's sensitivity, the adsorption parameter was the most important factor. The mod-
513 el was calibrated in order to achieve predictions that were close to the experimental data. A
514 reasonable agreement was obtained between the measured and predicted results. A mass
515 balance showed that up to 89%, 91% and 91% of the removal of HM was through adsorp-
516 tion, which is highly significant, whereas removal through the plants is about 6%, 5.1% and
517 5.2% for Pb, Cr and Cd, respectively. This study demonstrates that the developed mathe-
518 matical model could be used to describe the Pb, Cr and Cd removal process from landfill
519 leachate in the VFCW using ferric sludge.

520 Acknowledgements

521 Authors gratefully acknowledge the support of the technical staff at the Cardiff University
522 School of Engineering, in particular Mr. Jeff Rowlands. The first author would like to thank
523 the Iraqi Ministry of Higher Education and Scientific Research for financial support.

524 Referencies

- 525 Al-Tahmazi, T., Babatunde, A.O., 2016. Mechanistic study of P retention by dewatered
526 waterworks sludges. *Environ. Technol. Innov.* 6, 38–48. doi:10.1016/j.eti.2016.05.002
- 527 Bonanno, G., Lo Giudice, R., 2010. Heavy metal bioaccumulation by the organs of
528 *Phragmites australis* (common reed) and their potential use as contamination
529 indicators. *Ecol. Indic.* 10, 639–645. doi:10.1016/j.ecolind.2009.11.002
- 530 Cheng, S., Grosse, W., Karrenbrock, F., Thoennesen, M., 2002. Efficiency of constructed
531 wetlands in decontamination of water polluted by heavy metals. *Ecol. Eng.* 18, 317–
532 325. doi:10.1016/S0925-8574(01)00091-X
- 533 Galletti, A., Verlicchi, P., Ranieri, E., 2010. Removal and accumulation of Cu, Ni and Zn in
534 horizontal subsurface flow constructed wetlands: Contribution of vegetation and filling
535 medium. *Sci. Total Environ.* 408, 5097–5105. doi:10.1016/j.scitotenv.2010.07.045
- 536 Jørgensen, S.E., Fath, B.D., 2011. *Fundamentals of Ecological Modelling*, Fourth. ed,
537 *Developments in Environmental Modelling*. Elsevier, London.

538 Kadlec, R.H., Wallace, S.D., 2008. Treatment Wetlands, second edi. ed. New York.
539 doi:10.1201/9781420012514

540 Kosolapov, D.B., Kuschik, P., Vainshtein, M.B., Vatsourina, A. V., Wießner, A., Kästner, M.,
541 Müller, R.A., 2004. Microbial processes of heavy metal removal from carbon-deficient
542 effluents in constructed wetlands. *Eng. Life Sci.* 4, 403–411.
543 doi:10.1002/elsc.200420048

544 Kumar, J.L.G., Wang, Z.Y., Zhao, Y.Q., Babatunde, a O., Zhao, X.H., Jørgensen, S.E.,
545 2011. STELLA software as a tool for modelling phosphorus removal in a constructed
546 wetland employing dewatered alum sludge as main substrate. *J. Environ. Sci. Health.*
547 *A. Tox. Hazard. Subst. Environ. Eng.* 46, 751–757. doi:10.1080/10934529.2011.571600

548 Kumar, J.L.G., Zhao, Y.Q., 2011. A review on numerous modeling approaches for effective,
549 economical and ecological treatment wetlands. *J. Environ. Manage.* 92, 400–406.
550 doi:10.1016/j.jenvman.2010.11.012

551 Marchand, L., Mench, M., Jacob, D.L., Otte, M.L., 2010. Metal and metalloid removal in
552 constructed wetlands, with emphasis on the importance of plants and standardized
553 measurements: A review. *Environ. Pollut.* 158, 3447–3461.
554 doi:10.1016/j.envpol.2010.08.018

555 Mohammed, A., Al-Tahmazi, T., Babatunde, A.O., 2016. Attenuation of metal contamination
556 in landfill leachate by dewatered waterworks sludges. *Ecol. Eng.* 94, 656–667.
557 doi:10.1016/j.ecoleng.2016.06.123

558 Pimpan, P., Jindal, R., 2009. Mathematical modeling of cadmium removal in free water
559 surface constructed wetlands. *J. Hazard. Mater.* 163, 1322–1331.
560 doi:10.1016/j.jhazmat.2008.07.128

561 Stefanakis, A., Akrotos, C.S., Tsihrintzis, V.A., 2014. Vertical flow constructed wetlands: eco-
562 engineering systems for wastewater and sludge treatment, First edit. ed. Newnes, Lo.

563 Sun, G., Austin, D., 2007. Completely autotrophic nitrogen-removal over nitrite in lab-scale
564 constructed wetlands: Evidence from a mass balance study. *Chemosphere* 68, 1120–
565 1128. doi:10.1016/j.chemosphere.2007.01.060

566 Sun, G., Zhao, Y., Allen, S., 2005. Enhanced removal of organic matter and ammoniacal-
567 nitrogen in a column experiment of tidal flow constructed wetland system. *J. Biotechnol.*
568 115, 189–197. doi:10.1016/j.jbiotec.2004.08.009

569 van der Peiji, M.J., Verhoeven, J.T.A., 1999. A model of carbon, nitrogen and phosphorus
570 dynamics and their interactions in river marginal wetlands. *Ecol. Modell.* 118, 95–130.

571 Wang, J., Wang, X., Zhao, Z., Li, J., 2008. Organics and nitrogen removal and sludge
572 stability in aerobic granular sludge membrane bioreactor. *Appl. Microbiol. Biotechnol.*
573 79, 679–685. doi:10.1007/s00253-008-1466-6

574 Zhao, S.J., Zhang, Z.C., Gao, X., Tohsun, G., Qiu, B.S., 2009. Plant regeneration of the
575 mining ecotype *Sedum alfredii* and cadmium hyperaccumulation in regenerated plants.
576 *Plant Cell. Tissue Organ Cult.* 99, 9–16. doi:10.1007/s11240-009-9570-6

577 Zhou, Y.F., Haynes, R.J., 2011. Removal of Pb(II), Cr(III) and Cr(VI) from aqueous solutions
578 using alum-derived water treatment sludge. *Water. Air. Soil Pollut.* 215, 631–643.
579 doi:10.1007/s11270-010-0505-y